20th Australasian Fluid Mechanics Conference

Perth, Australia

5-8 December 2016

Nonlinear Internal Tide Dynamics on the Australian Northwest Shelf

N.L. Jones[1], C.E. Bluteau[1], G.N. Ivey[1], R. Dracup[1], J.W. Book[2] and A.E. Rice[2].

[1]School of Civil, Environmental and Mining Engineering & Oceans Institute,

University of Western Australia, Crawley 6009, Australia

[2]Naval Research Laboratory,

Stennis Space Center, Mississippi, 39529, USA

Abstract

The coastal shelf in Northwest Australia is a region of strong nonlinear internal wave generation and dissipation that results from strong tidal flows. Here we focus on moored observations collected in 100 m of water 4-22 April 2012. The moored instruments measured both mean vertical temperature and velocity structure as well as turbulence quantities at two point locations, 7.5 and 20.5 m above the seabed. The nonlinear internal wave (NLIW) packets were characterised by isotherm displacements of up to 60 m, occurred once per semi-diurnal tidal cycle and generally persisted for 4 h, with periods ranging from 10- 30 minutes. The NLIWs were not consistently phase-locked to either the surface tide. The largest turbulent overturns observed coincided with the downward isotherm movement of each of the NLIWs within a packet. The dissipation of turbulent kinetic energy was highest in the near-bed region during the passage of the largest amplitude NLIWs, coinciding with a strong shoreward mean current and pulse of cold water. Direct estimates of mixing from the moored turbulence instruments showed that shear and overturns resulting from the NLIW dynamics resulted in large increases in the dissipation of turbulent kinetic energy and vertical mixing. Our direct estimates of K_T demonstrate that using the traditionally employed Osborn model with a constant mixing efficiency can both vastly over-predict and under-predict the mixing rate.

Introduction

Internal waves on continental shelves can be important to both the local mixing and the global energy balance. Large non-linear internal waves (NLIW, or solitons) created by the surface tides may be a dominant contributor to vertical mixing and thereby play an important role in controlling the distribution of physical water properties, nutrient fluxes, and concentrations of particulate matter, e.g., [1].

Mixing on continental shelves has received comparatively little attention compared with the open ocean. Often it is assumed that bottom and surface boundary layer turbulence is of primary importance to vertical mixing in shelf waters, however, observations have shown that NLIWs can induce strong shear, enhanced dissipation and turbulent mixing in the interior of the water column [1].

Here we study the NLIWs and the turbulence characteristics on the Australian Northwest Shelf (NWS) over a 10 day period. We observe the temporal variation of the dissipation of turbulent kinetic energy ε and vertical diffusivity of heat K_T at 2 heights above the bottom during various conditions, including steep NLIWs.

Methodology

For three weeks in April 2012, the 35-m long BUBS mooring was deployed at the 105 m isobath (Figure 1). BUBS was instrumented with two moored turbulence packages (MTP) at 7.5 and 20.5 m above bed (mab). Each MTP consisted of an acoustic-Doppler velocimeter (ADV; Vector, Nortek-AS); fast-response temperature sensor (FP07, GE Thermometics) and a motion pack (MP; Rockland Scientific). The MP consisted of a 6 degrees of freedom motion sensor (O-navi, gyrocube); a micro-mag magnetometer to derive the instrument's heading once it's pitch and roll are reconstructed from the gyrocube data; and a fast-response pressure sensor. We used the MP data to remove the motion-induced contamination over the surface wave frequency band of the velocity and temperature measurements [2, 3]. These high-frequency turbulence measurements (8 Hz) provide estimates of the dissipation of turbulent kinetic energy ε and the dissipation of thermal variance χ_T via their respective inertial subranges [4]. Segments of 4096 data points (8.5 minutes) were used to estimate ε and χ_T. A total of 629 and 1532 estimates (from a possible total of 3293) of ε were made at 7.5 and 20.5 mab, respectively. The mooring was also instrumented with mean velocity, temperature (1 m spacing over 35 m) and conductivity sensors to derive the local mean shear S and stratification N. The vertical diffusivity of heat was estimated from

$$K_T = \frac{1}{2}\frac{\chi_T}{\left(\partial \bar{T} / \partial x_3\right)^2} \quad (1)$$

[5]. Here is $\bar{T}$ is the time-averaged temperature and x_3 is the vertical vertical direction. A total of 616 and 1677 estimates of K_T were made at 7.5 and 20.5 mab, respectively.

Barotropic velocities were estimated as the depth-average of the currents observed at the through water-column mooring (PIL100) located 200 m away in 100 m of water. Baroclinic velocities were defined as the difference between total and barotropic velocities.

Thorpe overturn length scales L_T, an estimate of the largest turbulent overturns, were estimated by reordering unstable overturns in instantaneous density profiles, which were extracted from 1 m vertically spaced temperature records. Only overturns that were larger than the accuracy of the sensors ($2 \times 10^{-3}°C$) were retained, therefore only inversions greater than $4 \times 10^{-3}°C$ were considered. Form these, we discarded overturns smaller than 5 m since the minimum resolvable overturn recommended by Galbraith and Kelley [6] is five-times the distance between sensors.

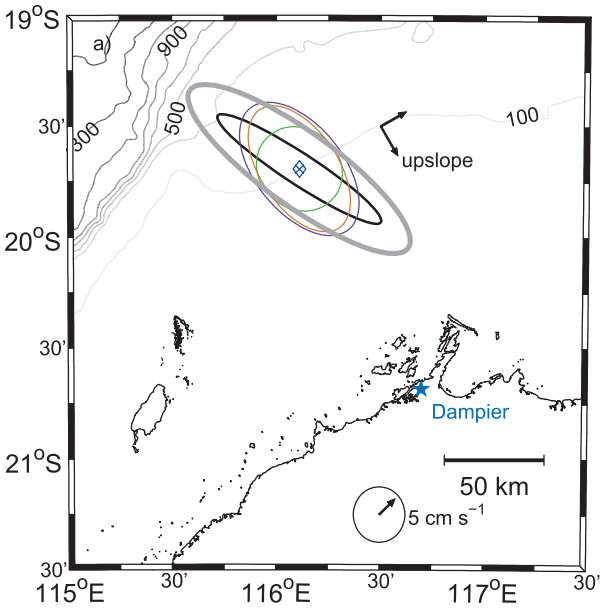

Figure 1 Regional bathymetry with the location of BUBS mooring (diamond), and the PIL100 mooring (X), and topographic up-slope direction indicated. The principal component ellipses are derived from PIL100 velocity: M2 barotropic ellipse (black); baroclinic ellipses at 10 mab (purple), 38 mab (green), and 84 mab (orange), and the depth-averaged total ellipse (grey).

Results and Discussion

Background conditions

During the three-week deployment, the total currents were as high as 0.8 ms^{-1} and propagated on average at 27° counter-clockwise from due east, almost aligning with the topographic slope at 60° counter-clockwise from due east (Figure 1). The main tidal constituents represented in the recorded velocities and pressure at PIL100 were M2, S2, K1 and O1, with the semidiurnal components dominating the diurnal constituents. Tidal amplitudes and velocities during spring tides exceeded 1.75 m and 0.5 m s^{-1}, respectively. The magnitude of the major axis, obtained via principal component analysis of the total depth-averaged velocity measured at PIL100, was ~0.25 m s^{-1}. This axis was aligned with the major axis of the M2 barotropic tide, but its magnitude was significantly larger (Figure 1). A net along-isobath flow towards the south-west was observed over the three week period. The background stratification estimated from the moored thermistors was nearly linear with a buoyancy period of about 9 minutes (Buoyancy frequency, N~10^{-3} rad s^{-1}).

On the NWS internal tides are generated offshore at the shelf-break [7]. The arrival of internal tides at the BUBS site was not phase-locked with the surface tide. Baroclinic velocities associated with the passage of internal waves were largest near the seabed. The nonlinear internal wave (NLIW) packets were characterised by isotherm displacements of up to 60 m, occurred once per semi-diurnal tidal cycle and generally persisted for 4 h, with periods ranging from 10-30 minutes, similar to those observed by Holloway et al. [8]. The NLIW events were generally stronger (larger amplitude and colder water) during neap tide compared with spring.

Turbulence and mixing

Thorpe length scales were log-normally distributed with a median value of 2 - 3 m. The largest Thorpe overturns of ~10 m or greater frequently coincided with the arrival of the first cold water front of each packet of NLIWs. The overturns associated with the following waves in the packet were generally much smaller (2-3 m). Larger Thorpe turbulent overturns coincided with the downward isotherm movement of each of the NLIWs within a packet.

The MTP recorded data for 9.5 days, capturing 20 NLIW events of various strengths. Turbulent kinetic energy dissipation ε at both the 7.5 mab and 20.5 mab MTPs ranged from 10^{-7} to $10^{-4.5}$ W kg^{-1} and was approximately lognormally distributed with median values of 1.4x10^{-6} and 9.9 x10^{-7} W kg^{-1} at 7.5 and 20.5 mab, respectively (Figure 2 top). There were a slightly larger proportion of higher ε values recorded at the MTP at 7.5 mab compared with 20.5 mab. The thermal mixing diffusivity K_T ranged from 10^{-5} to 10^{-1} m^{2}s^{-1} at both depths and was approximately lognormally distributed with median values of 1.9 x10^{-3} and 1.5x10^{-3} m^{2}s^{-1} at 7.5 and 20.5 mab, respectively (Figure 2 bottom). These median values are four orders of magnitude greater than the molecular value and the highest values are similar to those observed in internal tide beams in the open ocean, e.g., [9].

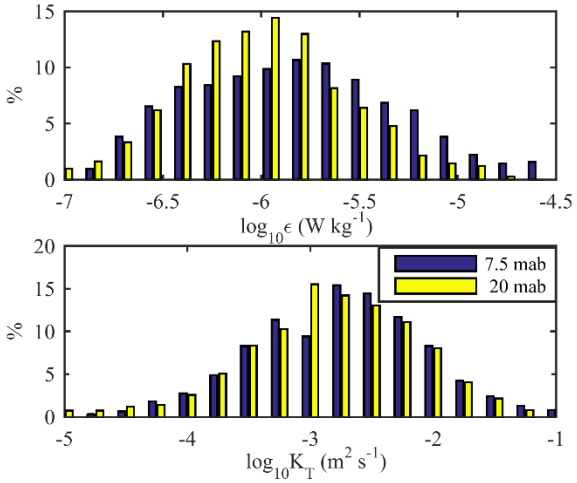

Figure 2 Histogram of ε (top) and K_T (bottom).

The highest values of ε and K_T generally coincided with the first arrival of cold water with each NLIW event when the largest Thorpe overturns were observed. However, we also observed high values of ε and K_T when there was sustained shear in the water column. Our observations indicate that the divergence of isopycnals does not seem to have had a large influence on the generation of turbulence at this site. To explore the relationship between NLIWs and mixing we present observations from two 6 h time periods.

The first example occurred during a neap tide period and illustrates a large increase in ε and K_T upon the arrival of cold water associated with a NLIW event when the largest Thorpe overturns were observed (Figure 3). The NLIWs arrived approximately 1 h after the surface tide turned to flood. Note that the NLIWs arrived at the PIL100 site approximately 0.25 h prior to their arrival at BUBS. The NLIWs were approximately 50 m in height and had a period of around 0.5 h. Large Thorpe overturns were observed during the hour-long period spanning the first two waves in the train. Prior to the arrival of the NLIWs, the ε values at each height were similar in magnitude. Upon the arrival of the cold water (time=2.5 h) ε was generally higher closer to the bed where the largest velocities were observed. Following the first two waves in the train of NLIWs the values of ε and K_T decreased to their lowest recorded values in this 6 h segment (time=3.8 h), despite corresponding with peak flood tide.

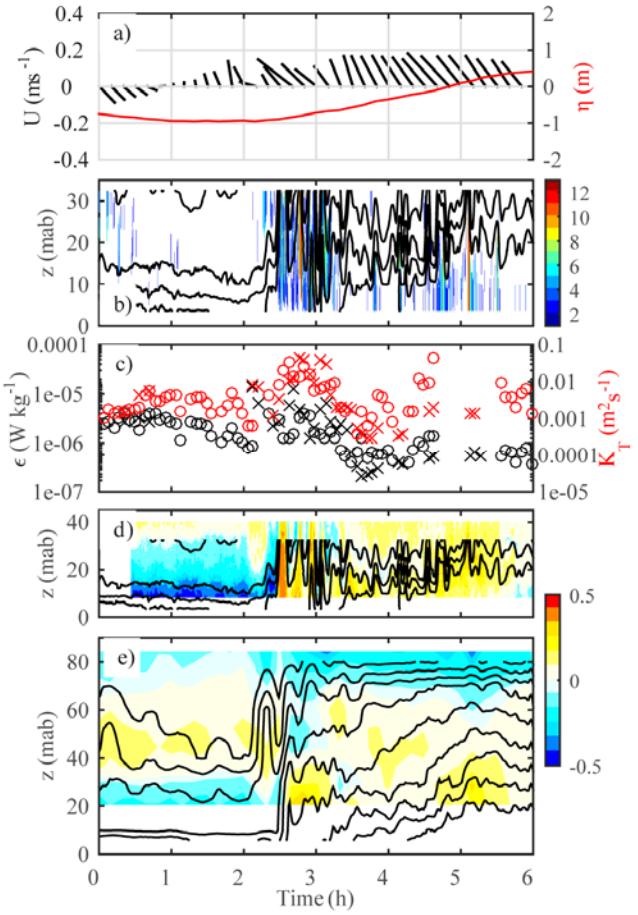

Figure 3 Six hour example of data from day 95. a) Surface tide velocity and elevation, b) Thorpe overturns (m, colours) and isotherms (0.5 ºC, back lines), c) ε and K_T at 7.5 mab (crosses) and 20.5 mab (circles), d) Cross-shore baroclinic velocity and isotherms at BUBS mooring, e) Cross-shore baroclinic velocity and isotherms at PIL100.

The second example is 24 h later than the first example and also occurred during neap tides (Figure 4). The baroclinic response is remarkably different with the near-bed cold water associated with the NLIWs only having a height of ~20 m and near-bed maximum baroclinic velocity of~0.1 m s^{-1}. The Thorpe overturn length scales were relatively small throughout the entire 6 h period. However, the values of ε and K_T were actually on-average larger than during the first example. Furthermore, ε was higher at 20.5 mab than at 7.5 mab for the first 2 h of the example. The large values of ε were associated with increased shear in the baroclinic velocity at ~20 mab as the thermocline was depressed to that height. The ε close to the bed increased with the arrival of the cold water. Similar to example 1, the observed ε was smallest following the passage of the NLIWs, however this time it corresponded with the beginning of the flood tide.

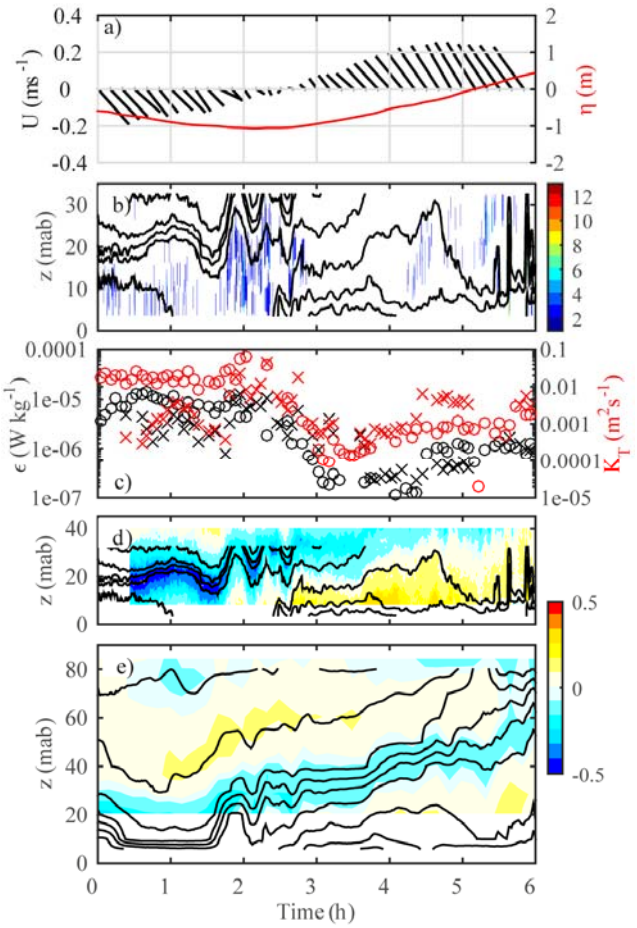

Figure 4 Six hour example of data from day 96. a) Surface tide velocity and elevation, b) Thorpe overturns (m, colours) and isotherms (0.5 ºC, black lines), c) ε and K_T at 7.5 mab (crosses) and 20.5 mab (circles), d) Cross-shore baroclinic velocity and isotherms at BUBS mooring, e) Cross-shore baroclinic velocity and isotherms at PIL100.

To determine if classic boundary log-layer theory, which assumes that shear production and ε are in balance, describes the turbulence dynamics at 7.5 mab we compared the observed ε to $u_*^3 / \kappa z$. Here u_* is the bed friction velocity, z is the height above the bed and von Karmen's constant κ=0.4. The bed friction velocity was predicted via the quadratic drag law

$$u_*^2 = C_d \mathbf{U}^2 \qquad (2)$$

Here C_d is the drag coefficient, which was set to the typical value of 1x10^{-3} and **U** is the total velocity vector at 7.5 mab. At 7.5 mab, over 50% of the ε estimates were greater than $10u_*^3 / \kappa z$, indicating that the turbulence was dominated by shear and mixing within the water column at this site.

The turbulent mixing rate is traditionally estimated via the Osborn model [10]

$$K_O = \frac{R_f}{1 - R_f} \frac{\varepsilon}{N^2} \qquad (3)$$

assuming the flux Richardson number is constant at R_f=0.17, e.g., [11]. We compared K_O to K_T, finding that 7% and 9% of K_O estimates were 1/3 or less of K_T at 7.5 mab and 20.5 mab, respectively (Figure 5). Furthermore, 28% and 10% of K_O estimates were over-predicted by 3 times or more compared with K_T at 7.5 mab and 20.5 mab, respectively. This highlights the

limitations involved with using the Osborn model with a simple constant mixing efficiency to estimate the mixing rate.

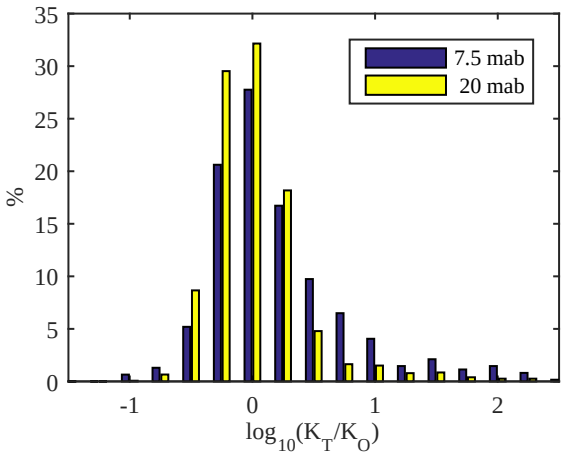

Figure 5 Histogram comparing the magnitude of mixing rates via equation (1) and equation (3) .

Conclusions

Our NWS observations illustrate the dynamic nature of the NLIW field and the resultant turbulence and mixing. The highest values of ε and K_T generally coincided with the arrival of cold bottom water with each NLIW event, when the largest Thorpe overturns were observed. However, we also observed high values of ε and K_T when there was sustained shear in the water column.

The observed values of ε at 7.5 mab were often not predicted by classic boundary layer theory, which assumes a balance between shear production and dissipation. Our direct estimates of K_T demonstrate that using the Osborn model (equation (3)) with a constant mixing efficiency can both vastly over-predict and under-predict the mixing rate. Our K_T estimates will ultimately be used to better parameterise stratified mixing.

Acknowledgements

An Australian Research Council (ARC) Discovery Projects (DP 140101322), an ARC Linkage Project (LP 110100017), an Office of Naval Research (ONR), Naval International Cooperative Opportunities Project (N62909-11-1-7058), an ONR project "AUV Data Analysis for Predictability in Time-Evolving Regimes" and an ONR project "Propagation and Dissipation of Internal Tides on Coastal Shelves" all contributed funding for this work. We thank people from the Australian Institute of Marine Science, the Naval Research Laboratory and the University of Western Australia who aided in the collection of the data and the crew of the RV Solander. The PIL100 data was sourced from the Integrated Marine Observing System (IMOS) -- IMOS is a national collaborative research infrastructure, supported by Australian Government.

References

1. MacKinnon, J.A. and M.C. Gregg, *Mixing on the late-summer New England Shelf—solibores, shear, and stratification.* Journal of Physical Oceanography, 2003. **33**(7): p. 1476-1492.

2. Bluteau, C.E., N.L. Jones, and G.N. Ivey, *Acquiring long-term turbulence measurements from moored platforms impacted by motion.* Journal of Atmospheric & Oceanic Technology, 2016.

3. Zhang, Y. and J.N. Moum, *Inertial-convective subrange estimates of thermal variance dissipation rate from moored temperature measurements.* Journal of Atmospheric & Oceanic Technology, 2010. **27**(11): p. 1950-1959.

4. Bluteau, C.E., N.L. Jones, and G.N. Ivey, *Estimating Turbulent Dissipation from Microstructure Shear Measurements Using Maximum Likelihood Spectral Fitting over the Inertial and Viscous Subranges.* Journal of Atmospheric and Oceanic Technology, 2016. **33**(4): p. 713-722.

5. Bluteau, C.E., et al., *Determining mixing rates from concurrent temperature and velocity measurements.* Geophys Res. Lett., under review.

6. Galbraith, P.S. and D.E. Kelley, *Identifying Overturns in CTD Profiles.* Journal of Atmospheric and Oceanic Technology, 1996. **13**(3): p. 688-702.

7. Bluteau, C.E., N.L. Jones, and G.N. Ivey, *Dynamics of a tidally-forced stratified shear flow on the continental slope.* Journal of Geophysical Research, 2011. **116**(C11): p. C11017.

8. Holloway, P.E., et al., *A nonlinear model of internal tide transformation on the Australian North West Shelf.* Journal of Physical Oceanography, 1997. **27**(6): p. 871-896.

9. Garrett, C. and L.S. Laurent, *Aspects of deep ocean mixing.* Journal of Oceanography, 2002. **58**(1): p. 11-24.

10. Osborn, T.R., *Estimates of the local rate of vertical diffusion from dissipation measurements.* Journal of Physical Oceanography, 1980. **10**(1): p. 83-89.

11. Waterhouse, A.F., et al., *Global patterns of diapycnal mixing from measurements of the turbulent dissipation rate.* Journal of Physical Oceanography, 2014. **44**(7): p. 1854-1872.